Educational Administration: Theory and Practice
2024, 30(1) 3947-3953
ISSN: 2148-2403
https://kuey.net/

Research Article

Preparation, Investigation of Physical and Chemical Properties, and Assessment of Biological Activity of Novel Metal Complexes of Benzilmonoximehydrazide Derivatives

Sharad Sankhe[1*] and Krupali Shah[1]

[1*]Department of Chemistry, Patkar-Varde College, Goregaon West, Mumbai-62, India.

Citation: Sharad Sankhe et al (2024), Preparation, Investigation of Physical and Chemical Properties, and Assessment of Biological Activity of Novel Metal Complexes of Benzilmonoximehydrazide Derivatives, *Educational Administration: Theory and Practice, 30(1) 3947-3953*
Doi: 10.53555/kuey.v30i1.7687

ARTICLE INFO

ABSTRACT

N-[(2E)-2-{[(4-chlorophenyl)methylidene]hydrazinylidene}-1,2-diphenylethylidene] hydroxylamine (HBMH*p*CB) is introduced as a potential chelating agent for binding with Fe(II), Ni(II), Co(II), Zn(II) and Cu(II) metal ions. The synthesized HBMH*p*CB ligand and its resulting metal complexes are characterized using various spectroscopic and analytical techniques including UV-vis, IR, ^{1}H NMR, powder XRD, ESR, magnetic, and conductance measurement. Analysis of spectral data indicates that the ligand coordinates to the metal ions in a tridentate manner through the oxygen and nitrogen atoms of the oximino group and the azomethine moiety. Analytical findings suggest a stoichiometry of 1:2 (metal: ligand) for all Cu(II) and Ni(II) complexes. Additionally, the normal magnetic moments observed for Fe(II), Co(II), Ni(II), and Cu(II) complexes support a high spin octahedral structure, while the diamagnetic behavior of all Zn(II) complex is consistent with tetrahedral geometry. Conversely, the subnormal magnetic values observed for Cu(II) complexes suggest a binuclear structural arrangement. ESR spectra of the Cu(II) complexes further indicate a distorted octahedral geometry with significant intrageneric spin-exchange interaction. Furthermore, the synthesized compounds are screened for antibacterial, and antifungal activities.

Keywords: Benzilmonoximehydrazide, octahedral structure, oximino group, tetrahedral geometry, diamagnetic behavior

Introduction:

Benzilmonoximehydrazide, also known as 2-hydroxy-1,2-diphenylethanone oxime hydrazide, is a chemical compound synthesized through the condensation reaction of benzil monoxime and hydrazine hydrate [1-5]. It is characterized by the presence of a hydrazide functional group (-$CONHNH_2$) attached to the benzil monoxime structure. This compound has attracted attention across various scientific domains including organic synthesis, coordination chemistry, and medicinal chemistry due to its inherent biological activities and reactivity [6-9]. Researchers explore its potential in diverse applications, from its utilization as a chelating agent in metal complexes to its investigation as a pharmacophore for designing new therapeutic agents [10-12]. The structural properties and chemical characteristics of benzilmonoximehydrazide make it a focal point of scientific inquiry, particularly in drug discovery efforts and other related research fields.

In the literature, studies have explored the synthesis methods for benzilmonoximehydrazide, emphasizing its potential as a versatile building block in organic synthesis. Researchers have investigated its reactivity towards different chemical entities, highlighting its role as a precursor in the formation of various functionalized compounds [13-15]. Moreover, benzilmonoximehydrazide has been extensively studied for its coordination chemistry properties. Research in this area has focused on its ability to act as a chelating ligand for metal ions,

leading to the formation of metal complexes with diverse structural and chemical characteristics. Spectroscopic and analytical techniques have been employed to elucidate the coordination modes and geometries of these complexes, providing insights into their potential applications in catalysis, materials science, and bioinorganic chemistry.

In the realm of medicinal chemistry, benzilmonoximehydrazide has emerged as a promising scaffold for the development of bioactive molecules. Studies have explored its pharmacological activities, including antimicrobial, antifungal, anticancer, and antioxidant properties. Structure-activity relationship (SAR) studies have been conducted to optimize its biological efficacy and selectivity, paving the way for the design and synthesis of novel therapeutic agents based on benzilmonoximehydrazide scaffold. Considering the aforementioned points, this paper focuses on the synthesis and spectroscopic characterization of complexes involving Fe(II), Ni(II), Co(II), Zn(II), and Cu(II) ions in conjunction with N-[(2E)-2-{[(4-chlorophenyl)methylidene]hydrazinylidene}-1,2-diphenylethylidene] hydroxylamine ligand as depicted in **Scheme 1**. This investigation aims to provide a detailed analysis of the spectral properties and structural features of these complexes. By examining the interactions between the metal ions and the ligands, valuable insights can be gained into their coordination behavior and bonding modes.

1. Experimental:

1.1. Materials, instruments, and methodology:

α-Benzilmonoximehydrazide (HBMOH) was synthesized via the condensation reaction between α-benzilmonoxime and hydrazine hydrate, following a previously reported protocol [16-18]. *p*-Chlorobenzaldehyde was procured from Sigma-Aldrich. The metal salts used in the synthesis of the complexes, including $FeSO_4$, $NiCl_2.6H_2O$, $ZnCl_2.7H_2O$, $CoCl_2.7H_2O$, and $CuCl_2.2H_2O$, were obtained from s. d. fine chem. All chemicals and solvents employed were of analytical reagent grade and were used without further purification. The melting points, recorded using a Digital Gallen-Kamp MFB-595 instrument, are reported without correction. Infrared spectra of the ligand and its metal complexes were measured using a Brucker FT-IR spectrometer with KBr discs, covering the range of 500–4000 cm^{-1}. Electronic spectral data of the solid complexes dissolved in DMF were obtained using a double-beam JASCO V650 UV–vis spectrophotometer within the wavelength range of 200-1000 nm. The molar magnetic susceptibility (meff) was determined at room temperature (296 K) using the Gouy method. Electron spin resonance (ESR) spectra were recorded with a JES-FE2XG-ESR Spectrometer (JEOL) operating at 8.7 GHz in a cylindrical resonance cavity with 100 kHz modulation. The g-values were determined by comparing them with the free radical DPPH (2,2-diphenyl-1-picrylhydrazyl) signal (g = 2.0037) [19]. The ^1H NMR spectra were recorded using a Bruker NMR 400 MHz Ultra ShieldTM in DMSO d_6. Chemical shifts are reported in parts per million (ppm) units. Elemental analyses (carbon, hydrogen, nitrogen, and sulfur) were performed by the Microanalytical Center, at Pune University.

1.1.1. Synthesis ofN-[(2E)-2-{[(4-chlorophenyl)methylidene]hydrazinylidene}-1,2-diphenylethylidene] hydroxylamine (HBMH*p*CB):

A heated solution comprising 10 mmol of benzilmonoximehydrazide dissolved in 100 mL of ethanol was supplemented with an ethanolic solution containing 12.50 mmol of *p*-chlorobenzaldehyde and 5 mL of concentrated hydrochloric acid. Following the completion of the reaction, the mixture was refluxed for five hours. Upon cooling, a yellow precipitate formed, which was subsequently filtered and washed with hot water. The resulting crude material underwent recrystallization from methanol, resulting in the isolation of pure HBMH*p*CB.

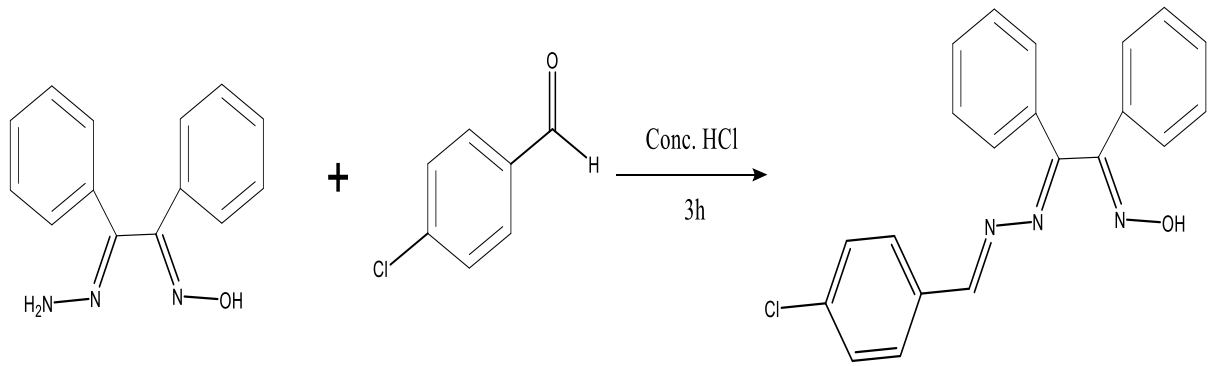

Scheme 1: Reaction scheme of HBMH*p*CB ligand

1.1.2. Transition metal complex synthesis:

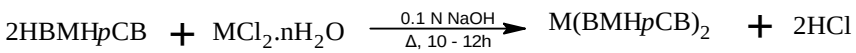

Scheme 2: Reaction scheme of metal complexes

1.2. Antimicrobial activity:

Multiple bacterial species, including *S. aureus, P. aeruginosa, B. subtilis*, and *E. coli*, were subjected to testing to characterize both the HBMH*p*CB ligand and its complexes. Additionally, the antifungal activity of the ligand was assessed against C. albicans and S. cerevisiae. Fluconazole served as the standard antifungal agent, while streptomycin was used as the common antibacterial agent [20]. Test solutions were prepared using dimethyl sulfoxide (DMSO). The efficacy of the compounds against bacteria was determined using the disc diffusion method. For each bacterial species under investigation, sterile agar medium was supplemented with 0.5 mL of spore suspension (containing 10^6 to 10^7 spores mL^{-1}) just before solidification. The mixture was then transferred into sterile Petri dishes with a diameter of 9 cm and allowed to solidify. Wells with a diameter of 6 mm were created in each plate using a sterile corn borer. Subsequently, three wells were filled with 0.1 mL of the tested substances dissolved in DMSO. The dishes were then incubated in an incubator set at 37°C for 48 hours (for bacteria) and 72 hours (for fungi) until clear or inhibitory zones formed around each well.

2. Results and Discussion:

The capacity of the synthesized HBMH*p*CB to engage in complex formation with various stoichiometric ratios is examined through various physico-chemical investigations, facilitated by the presence of multiple coordination sites. **Table 1** compiles key analytical and physical properties observed for the synthesized metal complexes. While certain organic solvents demonstrate insolubility in these compounds, they exhibit solubility in DMF, nitrobenzene, and DMSO.

Table 1: The HBMH*p*CB ligand and its metal complexes: analytical and physical data

Compound	Colour	Yield %	M.P. / Dec. point°C	Elemental Analysis						Magnetic Moments (B.M.)	Electrical Conductance 10^{-3} M(in NB) mhos
				% M Found (Calcd)	% C Found (Calcd)	% H Found (Calcd)	% N Found (Calcd)	% O Found (Calcd)	Cl% Found (Calcd)		
HBMH*p*CB	Yellow	76.55	188	-	69.69 (69.71)	4.42 (4.46)	11.59 (11.61)	4.41 (4.42)	9.70 (9.80)	-	-
[Fe(BMH*p*CB)$_2$]	Blue	69.87	201	7.18 (7.20)	64.90 (64.96)	3.85 (3.87)	10.80 (10.83)	4.11 (4.12)	9.12 (9.15)	5.63	0.18
[Co(BMH*p*CB)$_2$]	Brown	77.54	209	7.45 (7.57)	64.63 (64.70)	3.82 (3.85)	10.74 (10.78)	4.09 (4.11)	9.06 (9.11)	5.07	1.18
[Ni(BMH*p*CB)$_2$]	Green	79.88	211	7.50 (7.54)	64.60 (64.72)	3.83 (3.85)	10.76 (10.79)	3.83 (3.85)	9.01 (9.12)	3.19	1.69
[Cu(BMH*p*CB)$_2$]	Green	74.14	207	8.09 (8.11)	62.25 (62.32)	3.82 (3.83)	10.69 (10.72)	4.05 (4.08)	9.00 (9.05)	1.94	2.00
[Zn(BMH*p*CB)$_2$]	Yellow	71.36	208	8.28 (8.33)	64.11 (64.17)	3.77 (3.82)	10.66 (10.70)	4.02 (4.07)	9.03 (9.04)	-	0.33

2.1. FT(IR) spectra:

Table 2 presents the infrared spectral data. The free ligand displays a prominent broadband peak at 3047 cm^{-1}, attributed to the ν(N-OH) vibration of the oxime group. The absence of this characteristic in the complexes indicates deprotonation of the oxime hydroxyl group upon complex formation [21-23]. The distinct bands of the HBMH*p*CB ligand detected at 1566 and 1620 cm^{-1} were attributed to the oximino and azomethine groups, respectively. Upon complexation, these bands exhibited downward shifts, indicating the involvement of both groups in coordination processes [24-25].

This observation is further supported by the appearance of new bands at 552-659 cm^{-1} and 516-562 cm^{-1} in the complexes, corresponding to the stretching vibrations of ν(M-O) and ν(M-N) bonds, respectively [25-26]. Notably, there is no alteration in the absorption band of the ligand at 766-859 cm^{-1} associated with C-Cl, indicating that this group is not involved in coordination [27].

Table 2: The FT(IR) spectral bands of the ligand (HBMH*p*CB) and its metal complexes (cm^{-1}):

Assignments	νOH Oximino	νC=C Ar.	νC=NN	νC=NO	νN-N	C-Cl	νM-N	νM→N
HBMH*p*CB	3047	2995	1620	1566	1008	859	-	-
[Fe(BMH*p*CB)$_2$]	-	3025	1595	1537	1073	766	53	524
[Co(BMH*p*CB)$_2$]	-	3026	1597	1491	1091	819	659	516
[Ni(BMH*p*CB)$_2$]	-	3027	1593	1492	1039	822	558	540
[Cu(BMH*p*CB)$_2$]	-	2900	1595	1491	1089	821	620	562
[Zn(BMH*p*CB)$_2$]	-	2941	1588	1488	1085	812	552	520

2.2. ^{1}H-NMR spectra:

In the ^{1}H-NMR spectra, the phenyl groups corresponding to the aromatic region at 7.377-8.090 ppm are evident in both the HBMH*p*CB ligand and its Zn(II) complex. Notably, the singlet signal at 12.410 ppm, attributed to the N-OH proton, is absent in the Zn(II) complex of the HBMH*p*CB ligand, suggesting deprotonation of the oxime's hydroxyl group in the ligand [26].

Table 3: HBMHpCB ligand and complexes PMR spectrum

Compound	N-OH	=CH-	Aromatic Proton
HBMH*p*CB	12.410	10.592	7.377-8.090
[Pd(BMH*m*CB)$_2$]	-	10.398	7.370-8.116

2.3. Electronic spectra and magnetic moment:

The magnetic moments and electronic spectrum bands of the complexes are documented in **Table 1** and **Table 4**. Electronic spectra of HBMH*p*CB and its Fe(II), Co(II), Ni(II), Cu(II), and Zn(II) complexes in DMF exhibit absorption bands at 253-304 nm and 313-435 nm with high molar extinction coefficients, indicative of π→π* and n→π* intra-ligand charge transfer, respectively. These intense absorption bands satisfy Lapport selection requirements. Notably, the Fe(II) complex's electronic spectrum features broadband at 580 nm, likely arising from the $^5T_{2g} \rightarrow {}^5E_g$ transition. The consistent observation of octahedral geometry in complexes involving the ligand HBMH*p*CB and Fe(II) supports this finding.

The electronic spectra of the Co(II) complex in DMF reveal three medium-intensity bands at 900 nm, 610 nm, and 525 nm, assigned to the transitions $^4T_{1g} \rightarrow {}^4T_{2g}(F)$, $^4T_{1g} \rightarrow {}^4T_{1g}(P)$, and $^4T_{1g} \rightarrow {}^4A_{2g}(F)$. These values are explained using the effective symmetry of an octahedral environment. In the nickel(II) complex, the first and second ligand field transitions, $^3A_{2g} \rightarrow {}^3T_{2g}$ and $^3A_{2g} \rightarrow {}^3T_{1g}$, respectively, are observed at 980 nm and 630 nm. Using the Tanabe-Sugano diagram, parameters such as the Racah parameter, splitting energy, undetected third transition, and nephelauxetic parameter were calculated. Cu(II) with a d^9 structure anticipates an electronic transition from type $^2E_g \rightarrow {}^2T_{2g}$. The Cu(II) complex displays two Jahn-Teller distorted absorption bands at 690 nm and 604 nm, corresponding to the $^2B_{1g} \rightarrow {}^2B_{2g}$ and $^2B_{2g} \rightarrow {}^2E_g$ transitions, respectively. The observed magnetic moment of 1.94 B.M. in the Cu(II) complex aligns with that of octahedral Cu(II) complexes. Oximino and azomethine transition bands are observed in the 253-380 nm region of the electronic spectrum of the Zn(II) complex. Additionally, less intense and broader bands spanning 253-380 nm are attributed to the overlap between low-energy π → π* transitions, primarily located within the azomethine group, and ligand-to-metal charge transfer (LMCT) transitions originating from the lone pairs of the oximino oxygen donor to Zn(II).

Table 4: HBMH*p*CB ligand electronic absorption spectrum data and its metal complexes

Compound	λnm	ε (dm^3/mol/cm)	Transition
HBMH*p*CB	373	20520	π→ π*
	280	21431	π→ π*
[Fe(BMH*p*CB)$_2$]	580	129	$^5T_{2g} \rightarrow {}^5E_g$
	405	921	LMCT
	360	4520	LMCT
[Co(BMH*p*CB)$_2$]	900	6	$^4T_{1g}(F) \rightarrow {}^4T_{2g}(F)$ (ν_1)
	610	239	$^4T_{1g} \rightarrow {}^4T_{2g}$ (ν_2)
	525	446	$^4T_{1g}(F) \rightarrow {}^4T_{2g}(P)$ (ν_3)
[Ni(BMH*p*CB)$_2$]	980	12	$^3A_{2g}(F) \rightarrow {}^3T_{2g}(F)$ (ν_1)
	630	236	$^3A_{2g}(F) \rightarrow {}^3T_{1g}(F)$ (ν_2)
	540	518	$^3A_{2g}(F) \rightarrow {}^3T_{1g}(P)$ (ν_3)
[Cu(BMH*p*CB)$_2$]	690	741	$^2B_{1g} \rightarrow {}^2A_{1g}(d_{x2-y2} \rightarrow d^2_z)$ (ν_1)
	604	197	$^2B_{1g} \rightarrow {}^2B_{2g}(d_{x2-y2} \rightarrow d_{zy})$ (ν_2)
	510	2011	$^2B_{1g} \rightarrow {}^2E_g(d_{x2-y2} \rightarrow d_{zy}, d_{yz})$ (ν_3)
[Zn(BMH*p*CB)$_2$]	380	19521	LMCT
	304	21315	LMCT
	253	18968	LMCT

2.4. ESR Spectrum:

The EPR spectra of the Cu(II) complex were acquired from both a polycrystalline sample and a DMF solution. In both cases, the spectrum displays a distinctive anisotropic signal in both the parallel and perpendicular ^{63}Cu regions. Recorded data indicate $g_\perp$ values ranging from 2.0026 to 2.1306 and $g_{\square\square}$ values ranging from 2.0055 to 2.2301. According to [27], the copper(II) complex undergoes significant distortion from O_h symmetry to D_4h symmetry, as evidenced by g-values close to 2 and $g_{\square\square} > g_\perp > 2.0023$. The exchange interaction between copper centers in the polycrystalline solid was evaluated by computing a parameter $G = (g_{\square\square} - 2)/(g_\perp - 2)$. As per Hathaway [28,29], a G value greater than 4 suggests minor exchange contact,

whereas a G value less than 4 indicates a significant exchange interaction in solid complexes. The solid complexes investigated in this study exhibit significant exchange contact, as evidenced by G values smaller than 4.

2.5. Powder XRD:

X-ray diffraction patterns of the complexes were obtained in the 2θ = 20-80◦ range. The lack of peaks observed in the complexes indicates their amorphous nature [30].

2.6. Antimicrobial activity:

Table 5 presents the antibacterial and antifungal properties of the ligands and complexes. Enhanced activity is observed with higher concentrations of the test solution containing the complexes [31]. The antibacterial efficacy of the metal complexes surpasses that of the Schiff base ligands, as indicated in **Table 6**. Notably, among the complexes, the Cu(II) complex exhibits superior efficacy against both gram-positive and gram-negative bacteria. Furthermore, the fungicidal screening results in **Table 5** demonstrate that the Cu(II) and Ni(II) complexes display moderate activity compared to the other complexes and the Schiff base ligand.

Table 5: Antibacterial data of HBMH*p*CB ligand and its metal complexes

Compound	Antibacterial Activity (zone of inhibition)			
	S. aureus	***B. subtilis***	***E. coli***	***P. aeruginosa***
HBMH*p*CB	6	8	6	8
$[Fe(BMHpCB)_2]$	12	13	14	6
$[Co(BMHpCB)_2]$	15	12	15	13
$[Ni(BMHpCB)_2]$	17	14	17	15
$[Cu(BMHpCB)_2]$	15	14	14	12
$[Zn(BMHpCB)_2]$	19	20	18	17
Streptomycin	10	7	13	8

Table 6: Antifungal data of HBMH*p*CB ligand and its metal complexes

Compound	Antifungal Activity (zone of inhibition)	
	C Albican	*S. C.*
HBMH*p*CB	6	7
$[Fe(BMHpCB)_2]$	14	14
$[Co(BMHpCB)_2]$	15	19
$[Ni(BMHpCB)_2]$	17	15
$[Cu(BMHpCB)_2]$	12	10
$[Zn(BMHpCB)_2]$	11	12
Fluconazole	10	8

3. Conclusion:

The Schiff base ligand HBMH*p*CB is represented as $[ML_2]$ in the compounds formed by transition metal complexes. Based on the available data, L is confirmed to function as a tridentate ligand. The complexes formed with Fe(II), Co(II), Cu(II), and Ni(II) display octahedral geometry, while those with Zn(II) exhibit tetrahedral geometry. As per the results obtained from antibacterial assays, the Cu(II) complex demonstrates the highest efficacy among the tested metal complexes.

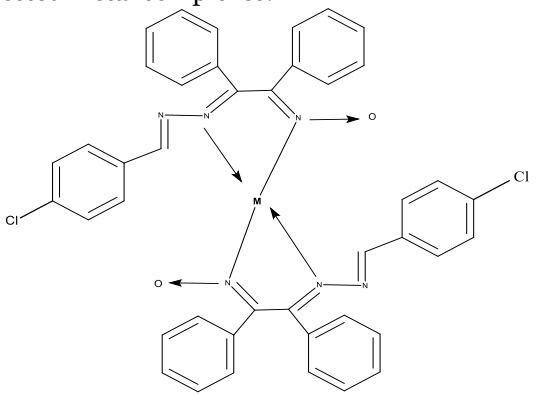

Where M = Fe(II), Co(II), Ni(II), Cu(II), and Zn(II)
Figure 1: Tentatively structures of the metal complexes

4. References:

1. Sharma, V. K., & Srivastava, S. (2005). Synthesis, Spectroscopic and Antifungal Studies of Trivalent Chromium, Manganese, Iron and Cobalt Complexes with Hydrazones Derived from Benzil α-Monoxime and Various Aromatic Hydrazides. *Synthesis and Reactivity in Inorganic, Metal-Organic and Nano-Metal Chemistry*, *35*(4), 311-318.
2. Mohammed, M. S. (2000). Spectrophotometric determination of some metal ions using hydrazones.
3. Taylor, T. W. J., Callow, N. H., & Francis, C. R. W. (1939). 54. The metallic derivatives of hydrazones and of the oxime-hydrazones of benzil. *Journal of the Chemical Society (Resumed)*, 257-263.
4. MONSHI, M. A., & ABDEL-SALAM, N. M. (1996). Metal Complexes of a Schiff Base formed by Condensation of S-Benzyl. *Jour. Chem. Soc. Pal;. Vol*, *18*(2).
5. Wieland, M., Seichter, W., Schwarzer, A., & Weber, E. (2011). Influence of different aryl substitution on the crystal structures of benzil monohydrazone and dibenzil azine parent compounds. *Structural Chemistry*, *22*, 1267-1279.
6. Malinowski, J., Zych, D., Jacewicz, D., Gawdzik, B., & Drzeżdżon, J. (2020). Application of coordination compounds with transition metal ions in the chemical industry—A review. *International Journal of Molecular Sciences*, *21*(15), 5443.
7. Mohammed, H. S., & Tripathi, V. D. (2020, November). Medicinal applications of coordination complexes. In *Journal of Physics: Conference Series* (Vol. 1664, No. 1, p. 012070). IOP Publishing.
8. Mawat, T. H., & Al-Jeboori, M. J. (2020). Synthesis, characterization, thermal properties and biological activity of coordination compounds of novel selenosemicarbazone ligands. *Journal of Molecular Structure*, *1208*, 127876.
9. Holló, B.B., Magyari, J., Armaković, S., Bogdanović, G.A., Rodić, M.V., Armaković, S.J., Molnár, J., Spengler, G., Leovac, V.M. and Szécsényi, K.M., 2016. Coordination compounds of a hydrazone derivative with Co (III), Ni (II), Cu (II) and Zn (II): synthesis, characterization, reactivity assessment and biological evaluation. *New Journal of Chemistry*, *40*(7), pp.5885-5895.
10. Manfrin, M. F., Moggi, L., Castelvetro, V., Balzani, V., Hosseini, M. W., & Lehn, J. M. (1985). Control of the photochemical reactivity of coordination compounds by formation of supramolecular structures: the case of the hexacyanocobaltate (III) anion associated with polyammonium macrocyclic receptors. *Journal of the American Chemical Society*, *107*(24), 6888-6892.
11. Comba, P. (2000). Coordination compounds in the entatic state. *Coordination Chemistry Reviews*, *200*, 217-245.
12. Boeckmann, J., Reinert, T., Jeß, I., & Näther, C. (2011). Syntheses, Structures, and Thermal Reactivity of New ZnII and CdII Thio-and Selenocyanato Coordination Compounds.
13. Soleimani, E. (2011). Synthesis and characterization of two novel complexes of Cr (III) with benzilmonoxime. *Journal of the Chinese Chemical Society*, *58*(1), 53-59.
14. Eskandari, H., Ghaziaskar, H. S., & Ensafi, A. A. (2001). A sensitive and simple extractive-spectrophotometric method for the determination of microgram amount of cobalt by using α-benzilmonoxime. *Analytical sciences*, *17*(2), 327-331.
15. Ganoub, N. A., Abdou, W. M., & Shaddy, A. A. (1998). THE reactions of alkyl phosphites with αβ-unsaturated carbon-nitrogen multiple-bonds: 2-benzylidenecyanomethyl-1, 3-benzothiazole and α-benzil monoxime. *Phosphorus, Sulfur, and Silicon and the Related Elements*, *132*(1), 109-122.
16. Badekar R, Lokhande R, Kulkarni S and Patil R; Synthesis and Characterization of (1E, 2E)-1, 2-Diphenylethane-1, 2-Diene Hydrazone Oxime ligand and its Fe(II) and Pd(II) metal complexes; *International Journal of Advanced Research;* **(2016),** 4, 8.
17. Badekar R, Lokhande R, Kulkarni S and Patil R; Synthesis and Characterization of α - Benzilmonoximehydrazone ligand and its Zn(II), Cd(II) and Hg(II) metal complexes; *International Journal of Advanced Research;* **(2016),**4, 7.
18. Badekar R, Badekar V, Kulkarni S, and Lokhande R; Studied on trivalent metal complexes of (1E, 2E)-1, 2-diphenylmethane-1, 2-diene hydrazone oxime ligand*; Golden Res Thought;* (**2016**), 1-12.
19. Davis, R. S. (1993). New method to measure magnetic susceptibility. *Measurement Science and Technology*, *4*(2), 141.
20. Zaidan, M. R., Noor Rain, A., Badrul, A. R., Adlin, A., Norazah, A., & Zakiah, I. (2005). In vitro screening of five local medicinal plants for antibacterial activity using disc diffusion method. *Trop biomed*, *22*(2), 165-170.
21. V. Fain, B. Zaitsev, M. Ryabov, P. Strashnov, *Russian Journal of General Chemistry*. **2010,** *80*, 1986-1995.
22. Z. Zhang, G. Helms, S. Clark, G. Tian, P. Zanonato, L. Rao, *Inorganic chemistry*. **2009,** *48*(8), 3814-3824.
23. E. Alvarez, J. Brodbelt, *Journal of the American Society for Mass Spectrometry*. **1998,** *9*(5), 463-472.
24. M. Odabaşoğlu, Ç. Albayrak, R. Özkanca, F. Aykan, P. Lonecke, *Journal of Molecular Structure*. **2007,** *840*(1-3), 71-89.
25. A. Sarwar, S. Saharin, H. Bahron, Y. Alias, *Journal of Luminescence*. **2020,** *223*, 117227.
26. I. Fritsky, R. Lampeka, V. Skopenko, Y. Simonov, A. Dvorkin, T. Malinowsky, *Zeitschrift für Naturforschung B*. **1993,** *48*(3), 270-276.

27. N. Hall, M. Orio, M. Gennari, C. Wills, F. Molton, C., Philouze, C. Duboc, *Inorganic Chemistry*. **2016,** *55*(4), 1497-1504.
28. T. Yamabe, K. Hori, T. Minato, K. Fukui, *Inorganic Chemistry*. **1980,** *19*(7), 2154-2159. https://doi.org/10.1021/ic50209a063.
29. L. Andrews, *The Journal of Chemical Physics*. **1968,** *48*(3), 979-982.
30. K. Buldurun, N. Turan, E. Bursal, A. Aras, A. Mantarcı, N. Çolak, I. Gülçin, *Journal of Biomolecular Structure and Dynamics*. **2021,** *39*(17), 6480-6487.
31. K. Buldurun, N. Turan, A. Savcı, N. Colak, *Journal of Saudi Chemical Society*. **2019,** *23*(2), 205-214.